Clays and Clay Minerals, Vol. 45, No. 1, 42–53, 1997.

TOPOLOGICAL AND THERMAL PROPERTIES OF SURFACTANT-MODIFIED CLINOPTILOLITE STUDIED BY TAPPING-MODE™ ATOMIC FORCE MICROSCOPY AND HIGH-RESOLUTION THERMOGRAVIMETRIC ANALYSIS

E.J. SULLIVAN,[1] D.B. HUNTER[2] AND R.S. BOWMAN[1]

[1]Department of Earth and Environmental Science and Geophysical Research Center, New Mexico Institute of Mining and Technology, Socorro, New Mexico 87801

[2]Division of Biogeochemistry, University of Georgia, Savannah River Ecology Laboratory, Aiken, South Carolina 29801

Abstract—Unmodified and surfactant-modified clinoptilolite-rich tuff (referred to here as "clinoptilolite") and muscovite mica were examined with tapping-mode atomic force microscopy (TMAFM) and high-resolution thermogravimetric analysis (HR-TGA) in order to elucidate patterns of hexadecyltrimethylammonium bromide (HDTMA) sorption on the treated surface and to understand the mechanisms of this sorption. TMAFM images were obtained to a scale of 50 nm by 50 nm. The images of unmodified clinoptilolite showed a framework pattern on the *ac* plane, comparable to previously reported images. Images of modified clinoptilolite at 12.5% and 25% of external cation exchange capacity (ECEC) coverage by HDTMA showed evidence of the HDTMA molecules arranged as elongated, topographically raised features on the *ac* plane. At 50% HDTMA coverage, the images contained what appeared to be agglomerations of surfactant tail groups. The *z*-direction thickness of the raised features on the 12.5% coverage sample corresponded to the thickness of the carbon chain of the surfactant tail-group (0.4 nm), whereas the *z*-thickness on the 25% coverage sample was between 0.4 and 0.8 nm, indicating crossing or doubling of tail groups. Repulsive forces between the modified clinoptilolite and the silicon TMAFM probe increased with increasing HDTMA coverage. HR-TGA showed a 100 °C increase in HDTMA pyrolysis temperatures at coverages of less than 50%, probably due to an increased stabilization of the HDTMA due to direct tail interactions with the clinoptilolite surface at lower coverages versus smaller stabilization due to surfactant tail-tail interactions at higher coverages. Our results indicate that buildup of HDTMA admicelles or some form of a bilayer begins before full monolayer coverage is complete.

Key Words—Hexadecyltrimethylammonium, Muscovite Mica, Surface Imaging, Thermal Analysis, Zeolite.

INTRODUCTION

Surfactant-modified clay minerals, particularly bentonites, are undergoing extensive study because of their potential use as environmental sorbents. Zeolite minerals have surface chemistries similar to clays, but display superior hydraulic properties. Surfactant-modified clinoptilolite-rich tuff (referred to here as "clinoptilolite") was shown in batch sorption studies to be an effective sorbent of both nonpolar organic compounds and inorganic anions from water (Bowman et al. 1995; Haggerty and Bowman 1994; Neel and Bowman 1992). While the mechanism of organic sorption appears to be partitioning, the mechanism of inorganic anion sorption is not clear. To understand both mechanisms, we utilized TMAFM and HR-TGA to characterize HDTMA sorption on clinoptilolite. The TMAFM gave direct information about the placement of the surfactant on the clinoptilolite surface, whereas HR-TGA indicated intermolecular interactions between surfactant and clinoptilolite and between neighboring surfactant molecules.

Cationic surfactants, such as HDTMA, exchange with native cations such as Na^+, K^+ or Ca^{2+} on the clinoptilolite surface, producing an organic carbon-enriched surface (Haggerty and Bowman 1994). Large surfactants are excluded from the interior channels of the clinoptilolite and, thus, exchange only with cations on the exterior of the crystal. The HDTMA molecule consists of a 16-carbon chain tail group attached to a 3-methyl quaternary amine head group with a permanent 1+ charge. It is water-soluble and exists as monomers in solution below the critical micelle concentration (CMC) or as micelles above the CMC of 9×10^{-4} *M* at 25 °C (Israelachvili 1991). Summation of the van der Waals packing radii for a 3-methyl ammonium head group yields a diameter of 0.694 nm. A fully-extended HDTMA chain length of 3.5 nm can be calculated by adding the effective van der Waals radii for the appropriate number of $-CH_2$ and $-CH_3$ groups (Israelachvili 1991). A typical carbon chain diameter of 0.4 nm can also be calculated from the packing radii (Israelachvili 1991). The HDTMA molecule is large compared with the clinoptilolite cage structure and surface topography and is, thus, a good candidate for observation by TMAFM. The mean aggregation number of the micelles, based on head group area, was calculated to be about 95 monomers per micelle, assuming a spherical micelle (Israelachvili 1991). Al-

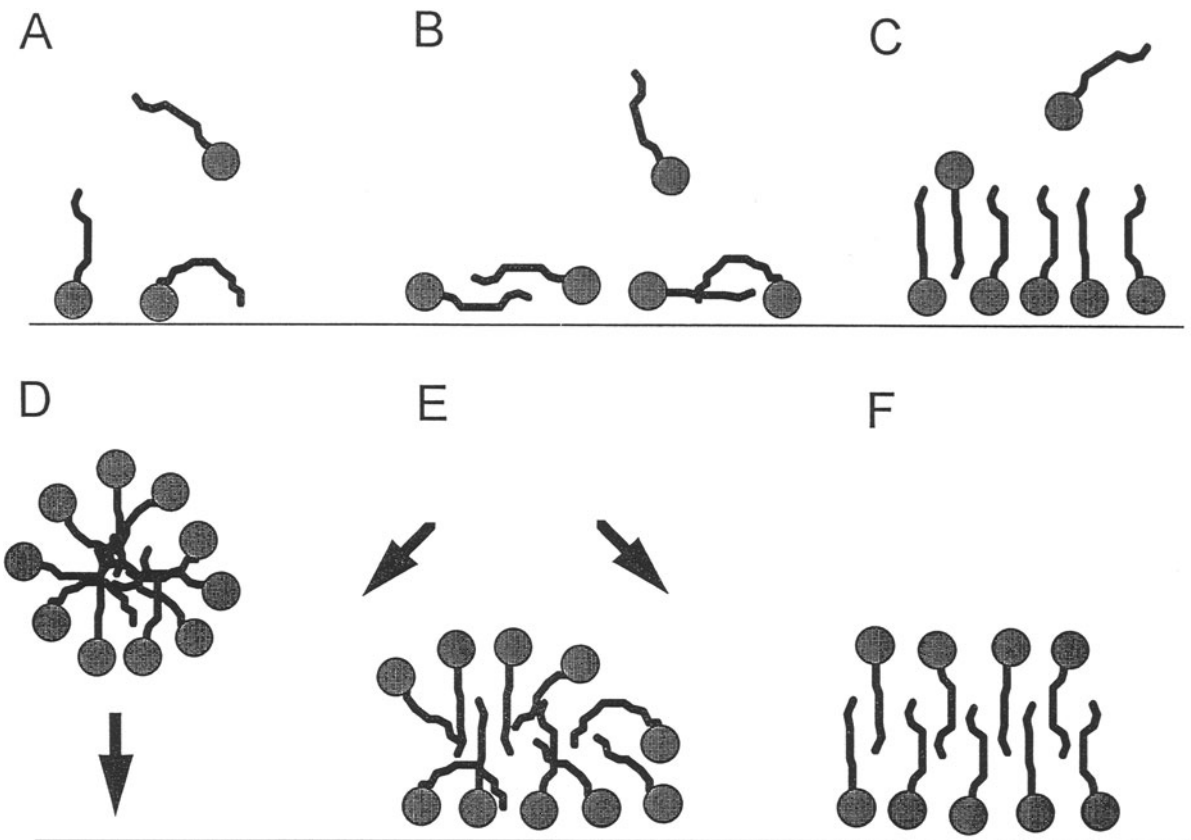

Figure 1. Concept of monomer, bilayer and admicelle sorption on mineral surfaces. A) and B) show potential monomer conformations after sorption. C) shows beginning development of a bilayer from monomer sorption. D) through F) show admicelle sorption, rearrangement and bilayer development when the solution is above the critical micelle concentration (adapted from Chen et al. 1992.)

though this value can vary with temperature and concentration, it is well within published ranges (Reiss-Husson and Luzzati 1964; Malliaris et al. 1986).

Sorption of ionic surfactants onto a charged solid surface can proceed by at least 2 pathways, depending upon surfactant concentration in solution. Below the CMC, surfactant monomers are sorbed, eventually developing a monolayer or a bilayer configuration, depending upon the amount of surfactant available (Figures 1a through 1c). Monomers sorb individually by coulombic interactions to available exchange sites and also by hydrophobic tail group interactions. Chen et al. (1992) presented a model of sorption of HDTMA to muscovite above the CMC. Micelles rapidly sorb to the surface and rearrange as space and charge permit (Figures 1d through 1f). A loosely packed bilayer is formed, growing to form a more densely packed bilayer. As the surface coverage increases, rearrangement slows. The hydrophilic micelles are less attracted to the increasingly hydrophobic surface, the release of the charge-balancing ions, such as Na^+ surface ions and Br^- counterions, is slowed through the bilayer and slower growth toward the equilibrium bilayer arrangement occurs. Rearrangement and micelle sorption continue, based on electroneutrality, up to equilibrium.

Manne and Gaub (1995) presented an alternate to this final arrangement on the mineral surface. They used non-contact-mode AFM to observe tetradecyltrimethylammonium on mica surfaces. Instead of rearrangement of the sorbed micelles to a bilayer, they noted the formation of linear features which were interpreted as elongated, tubular-type micelles. The features were mostly parallel-lying, with some random scattering.

AFM produces molecular-scale images of non-conducting substrates and has been used successfully to characterize zeolites at scales from 10 μm to 5 nm. Large crystals (>50 μm) of clinoptilolite are uncommon, and thus, studies of the mineral structure and surface are difficult at best (Smyth et al. 1990). To date, the reported AFM studies of zeolites describe macrocrystalline zeolites that were artificially cleaved; the present study, however, is concerned with microcrystalline clinoptilolite. Previous images produced with contact-mode AFM showed a repeating pattern comparable to unit-cell dimensions. Komiyama and

https://doi.org/10.1346/CCMN.1997.0450105 Published online by Cambridge University Press

Yashima (1994) imaged heulandite (isostructural with clinoptilolite) in air. Their images showed corrugations as they approached atomic resolution, but the structure did not match with crystallographic data. Scandella et al. (1993) found a similar framework structure on the *ac* plane of heulandite with contact-mode AFM. They also noted that the surface unit-cell measurements were 26% larger than the bulk unit-cell measurements made by X-ray diffraction (XRD). Weisenhorn et al. (1991) used contact-mode AFM with a fluid cell to image an artificially cleaved clinoptilolite surface that had been exposed to tert-butanol or tert-butyl ammonium ion. They observed a framework pattern comparable to repeating clinoptilolite unit cells. Clusters of tert-butanol molecules were observed on the clinoptilolite surface, but no clustering of the tert-butyl ammonium was detected.

We imaged at the near-molecular scale to view the distribution, conformation and *x, y* and *z* dimensions of the HDTMA molecules on the clinoptilolite surface. The studies cited above used contact mode AFM, in which the tip is in continuous contact with the surface. This method has the disadvantage of applying lateral forces that can disturb fragile sample surfaces. Contact-mode AFM on dry samples often results in high repulsive forces between the probe and surface, which can damage the surface and limit resolution (Zhong et al. 1993; Maurice 1995). In TMAFM, an applied voltage oscillates the probe so that it taps the surface many times for each data point. This produces extremely high resolution by reducing net repulsive and lateral forces to the range of 0.1 to 1 nanonewton (nN), preserving the probe and minimizing surface distortion (Zhong et al. 1993; Maurice 1995). Oscillation voltages can be varied to overcome repulsive forces from mineralogical changes, surfactant coatings or other surface-probe interactions. The present study shows that TMAFM can be used to image sequential sorption of HDTMA onto a microcrystalline clinoptilolite surface. Molecular-scale images (to 50 nm) were obtained in air for clinoptilolite and surfactant-modified clinoptilolite, as well as for surfactant-modified muscovite as a comparison. We observed the surface structure of the unmodified clinoptilolite and the conformation of HDTMA on clinoptilolite and muscovite. We also measured the dimensions of HDTMA molecules on clinoptilolite and muscovite surfaces. An empirical estimate of modified clinoptilolite surface properties derived from TMAFM set-point values is presented.

We compared the quantities of HDTMA sorbed via batch studies with the results of the HR-TGA analysis. HR-TGA is improved over previous thermal methods by the computerized correlation of temperature changes with measured weight loss. As discrete weight losses occur, the temperature is held constant until the loss is completed. TGA is widely used in the analysis of zeolites (Bish 1988; Ming and Mumpton 1989). HR-TGA pyrolysis temperatures should be higher for samples with more strongly bound HDTMA, such as that bound with both coulombic and van der Waals forces at sub-monolayer coverages (Figure 1a). If some of the HDTMA is bound only with hydrophobic forces, such as in a bilayer (Figure 1f), the pyrolysis temperatures should be considerably lower. Here we present HR-TGA data showing the temperatures of water desorption and the pyrolysis and subsequent desorption of HDTMA. Desorption derivative peaks were correlated with breakdown of HDTMA in the outer and inner parts of the surface bilayer or admicelles.

MATERIALS AND METHODS

Materials

The zeolite used is a clinoptilolite-rich tuff from the St. Cloud mine in Winston, New Mexico. It consists of about 74% clinoptilolite, 5% smectite clay, 10% quartz and cristobalite, 10% feldspar and 1% illite, based on internal standard XRD analysis (J. W. Carey, Los Alamos National Laboratory, personal communication, 1995; Chipera and Bish 1995). We measured an ECEC of 70 to 90 meq/kg for the St. Cloud clinoptilolite using the method of Ming and Dixon (1987). We also measured an external surface area of 15.7 $m^2\ g^{-1}$ on a sample dried for 24 h at 200 °C. The analysis was performed with an ASAP 2000 surface area analyzer (Micromeritics, Inc., Norcross, Georgia) using the BET nitrogen adsorption method (Brunauer et al. 1938). The surfactant used for clinoptilolite surface modification was HDTMA bromide of greater than 99% purity (Sigma Chemicals). Muscovite mica (Ted Pella, Inc., Redding, California) was freshly cleaved, treated with HDTMA and imaged for comparison with the modified clinoptilolite. All aqueous solutions were made with 18.2 Mohm cm^{-1} (ASTM Type I) water.

Surfactant Modification

The clinoptilolite was saturated with sodium to ensure a uniform substrate by shaking 40 g of clinoptilolite for three 15-min rinses with 120 mL of 1 *N*, pH 5 sodium acetate buffer in a 500-mL polypropylene centrifuge bottle. The samples were centrifuged at 14,500 × g, the supernatant discarded and the entire sequence repeated 2 more times. This was followed by 3 rinses with Type I water and 3 rinses with 95% ethanol, then air drying.

The sodium-saturated clinoptilolite was modified with surfactant to 0, 12.5, 25, 50, 100 and 200% of its ECEC, where 100% was assumed equal to 70 meq/kg clinoptilolite. Surfactant modification consisted of shaking 5 g of clinoptilolite with 20 mL of the selected HDTMA solution for 12 h at 25 °C in a 50-mL polypropylene Oak Ridge centrifuge tube. This amount of

time was shown to be sufficient for complete reaction of HDTMA on clinoptilolite (Sullivan et al. 1994). All solutions were well above the HDTMA CMC of 9×10^{-4} *M*. The HDTMA-modified clinoptilolite was centrifuged at 14,500 × g and excess HDTMA solution decanted. The clinoptilolite was placed on a polypropylene filter in a Buchner funnel, rinsed with 3 to 5 mL of Type I water and air-dried prior to analysis by TMAFM and HR-TGA. Appropriate blanks without clinoptilolite or HDTMA were also prepared.

The muscovite was cleaved to expose a fresh surface, immersed in a 5×10^{-4} *M* aqueous HDTMA solution for 10 min, removed and allowed to air dry before TMAFM.

Tapping-mode Atomic Force Microscopy

Sample mounts for the TMAFM were prepared by peeling a thin layer of dried clinoptilolite from the filter and attaching the peel to a magnetic sample disc with double-sided adhesive. This method ensured that no adhesive was imaged or could damage the TMAFM probe. Modified muscovite sheets were mounted with adhesive and trimmed to fit the mounting disc.

A Nanoscope III Scanning Probe Microscope station operating a Multi-Mode Atomic Force Microscope (Digital Instruments, Santa Barbara, California) was used in TappingMode™ for all scans. The microscope was equipped with a 12-μm nominal maximum scan-range scanner and 125-nm diameter silicon Nanoprobes. Scan rate and set-point voltages were adjusted for each sample as appropriate. Scan rates ranged from approximately 0.8 to 2 Hz. Relative humidity at the time of scanning was approximately 50%. Imaging was performed at the lowest possible tip pressure (set point), which was adjusted by retracting the tip until the surface was disengaged, then gradually readvancing the tip until the surface was contacted with minimum pressure. Scanned areas ranged from 8 μm by 8 μm square to 50 nm by 50 nm square. Each sample was scanned in a series from larger to smaller scan size while maintaining the beginning *x*–*y* coordinates, with areas of interest selected from the previous scan. This way, locations on specific crystal faces and specific features of interest could be correlated among different images. This method reduced the likelihood of mistaking noise or resonant frequencies for actual surface features. Most images were scanned at a resolution of 512 data points per scan line. Some images were scanned at 256 points per line.

Post-image processing was kept to a minimum. Low-pass filtering was applied to most sample images and did not affect the features of the images. Some images were flattened to resolve the *z*-scale, and some were very slightly contrast-enhanced to improve clarity. The flattening and contrast enhancement also did not affect the features of the images except to bring forward darkened areas at the edges of the scanned region. This was necessary due to the low microscopic topography encountered in some samples. The shading of the *z*-scale was adjusted as appropriate for each image depending upon topography. Surface topography was measured with the image processing software provided with the Nanoscope system. Horizontal and relative vertical measurements were made from point to point on the screen using the mouse and cursor. At least 20 relative vertical scale measurements were chosen from the *x, y, z* data files for each image of modified clinoptilolite or modified muscovite to measure the thickness of the HDTMA imaged on the surface. Relative *z*-values given here are the average values.

High-resolution Thermogravimetric Analysis

HR-TGA was performed on a Hi-Res™ TGA 2950 (TA Instruments, New Castle, Delaware). Approximately 10 mg of dried, modified or unmodified clinoptilolite were placed on a platinum micro-balance pan. The oven was purged with He gas, and the clinoptilolite weight loss was measured from 30 to 900 °C. Optimum resolution was obtained with a resolution setting of 4 and a sensitivity setting of 4. These 2 parameters permit adjustment of the equipment's patented feedback algorithm. The resolution setting adjusts the temperature ramp in response to a weight change, whereas the sensitivity setting adjusts when a weight changed is detected. Both these parameters are relative to the preset temperature ramp rate. These parameters are empirical and optimal settings are arrived at by repeated trials. We used weight loss vs. temperature curves and the resulting derivative curves in our analysis. The derivative of the weight loss curve was calculated at 2.5 °C min^{-1} smoothing.

RESULTS AND DISCUSSION

Low-resolution TMAFM Images

Unmodified clinoptilolite samples at the 1.25-μm scale (Figure 2) exhibited well-defined, monoclinic crystals with excellent crystal faces, and well-defined crystal edges in the *ac* plane. Small crystal fragments which had adhered to the flat crystal faces and edges were observed. Step heights of 65.7, 35.7 and 17.5 nm were measured, which closely correspond to multiples of the 17.9-nm *b*-spacing of a unit cell. Figure 2 also clearly shows crystals with a β angle of 116°. These images are comparable to microprobe or electron microscopy images in quality and scale.

As surface coverage of HDTMA increased, smaller, more agglomerated crystals and more poorly defined crystal edges were noted in the 1-μm (approximate) scale samples (Figure 3). The apparent sharpness of the images decreased with increasing surfactant coverage. In addition, increased topography was noted, and fewer flat crystal surfaces were available for imaging. Some samples showed a buildup of striated sur-

https://doi.org/10.1346/CCMN.1997.0450105 Published online by Cambridge University Press

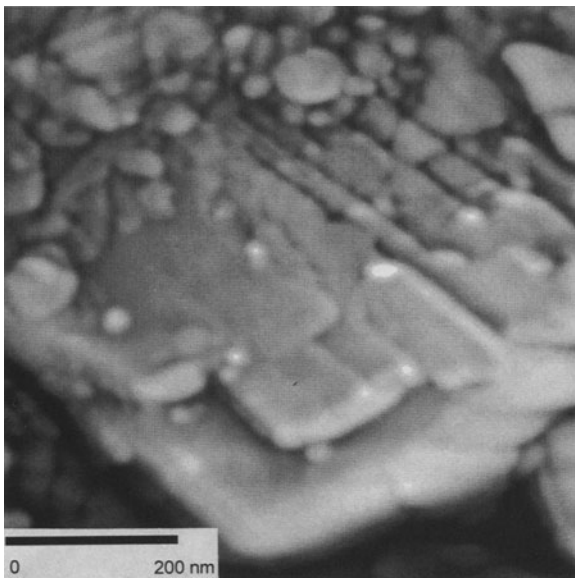

Figure 2. Unmodified St. Cloud clinoptilolite, 1.25-μm by 1.25-μm scale.

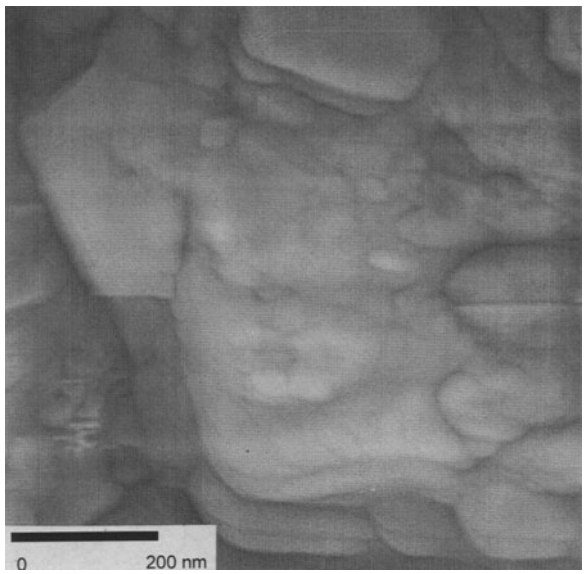

Figure 3. Clinoptilolite modified to 25% of ECEC with HDTMA, 1-μm by 1-μm scale.

factant material at and above 50% coverage (Figure 4). These features are likely clusters of HDTMA molecules lying on the surface. It is unlikely that the features are the result of dragging of HDTMA material by the TMAFM probe because of the low pressure exerted by the probe on the surface and because the striations appear to follow the orientation of the crystal surface, not the left-to-right probe scan direction. These linear features lie along different directions for different crystals, indicating that they may be controlled by the underlying structure of the crystal. The surfaces appear to be completely covered with these features. When they are distinct, they are similar to linear features reported by Manne and Gaub (1995) on mica, which were spaced 5.3 nm apart. The ridge-like features here are about 5 to 9 nm wide and are separated by about 5 to 9 nm wide spaces. At 100% treatment, the crystals are more rounded and less distinct (Figure 5). Flat surfaces and cleavage planes are less visible, although small crystals can still be seen. In the 200% coverage image (Figure 6), there appears to be excess buildup of HDTMA at the edges of crystal cleavage planes or steps. Additional exchange sites may be available in these locations due to the exposure of parts of the interior channel structure.

High-resolution TMAFM Images

A distinct, reproducible, grid-like pattern was noted on the unmodified sample (Figure 7) and also on the 12.5% and 25% modified samples at the 50 nm by 50 nm scale (Figures 8 and 9). No pattern was distinguishable at higher treatment levels (Figure 10). The grid spacing varied in scale slightly between images, most likely due to the angle of the crystal and tip interaction. The grid pattern can be compared to previously published clinoptilolite images of the *ac* plane from contact-mode microscopy under fluid (Scandella et al. 1993; Weisenhorn et al. 1991). Those images, however, were of large (1.9 × 1.2 mm) crystals that had been artificially cleaved while these are of uncleaved, air-dried crystals. Topographic features at this scale are controlled by the shape of the repulsive electron clouds (Stipp et al. 1994) and are to some extent a convolution of the shape of the tip and the surface

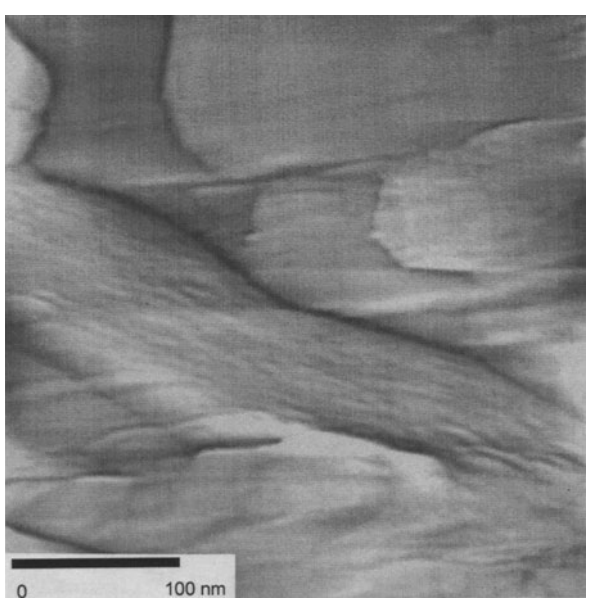

Figure 4. Clinoptilolite modified to 50% of ECEC with HDTMA, 1-μm by 1-μm scale.

https://doi.org/10.1346/CCMN.1997.0450105 Published online by Cambridge University Press

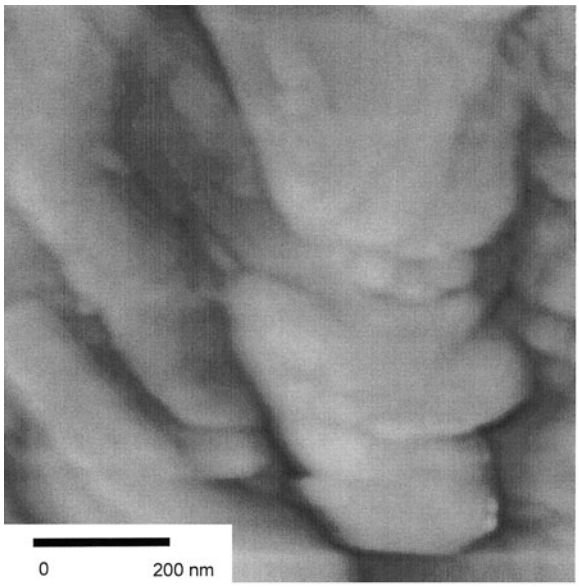

Figure 5. Clinoptilolite modified to 100% of ECEC with HDTMA, 1-μm by 1-μm scale.

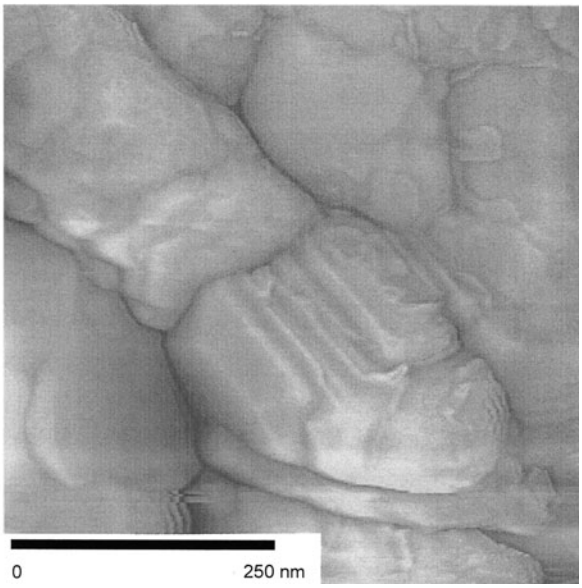

Figure 6. Clinoptilolite modified to 200% of ECEC with HDTMA, 1-μm by 1-μm scale.

topography, although this is minimized by tapping mode (MacDougall et al. 1991; Zhong et al. 1993). The high points correspond to electron-dense sites, such as the hydroxyl groups, that form at cleavage sites on the *ac* plane, and also correspond to some framework oxygen locations. The pattern is interpreted to be an expression of these hydroxyl groups or oxygens which extend slightly above the *ac* plane.

HDTMA appears on the surface of the clinoptilolite as elongated zones or linear features that obscure the surface grid pattern (Figures 8, 9 and 10). The size of these features on the 12.5% treatment sample is about 20 nm in length, 2 nm across and 0.4 nm high in relation to the adjacent clinoptilolite surface, based on a number of measurements made from the *x, y* and *z* data file. These features are several times longer, but about the same *z*-dimension, as the most elongated possible dimension of an HDTMA molecule (3.5 nm long by 0.4 nm diameter), and wider than the average HDTMA micelle diameter of approximately 4.3 nm (Israelachvili 1991). These features are probably horizontally oriented clusters of surfactant molecules. A single micelle with an aggregation number of 95, when rearranged to a monolayer, could cover about 83 nm^2 on the surface with closely packed HDTMA molecules (Israelachvili 1991), about double the observed feature size. The *z*-dimension of the features is an indication that the HDTMA tail groups are lying close to the surface. In these images, HDTMA appears sorbed in elongated clusters, rather than regularly distributed across the surface or in rounded areas, which might be expected from symmetrical micelle spreading. This may be an indication of the distribution of cation exchange sites on the surface, rearrangements of the surfactant due to agitation during the equilibration process or other effects, such as attractive forces between HDTMA tail groups. On the 25% treatment sample (Figure 9), the linear features are thicker (approximately 0.8 nm) and are almost fully covering the grid pattern on the surface. At 50% treatment (Figure 10), no grid pattern was obtainable and the surface appears coated with linear agglomerations of HDTMA. No reference surface was visible to measure the *z*-dimension of the HDTMA at 50% treatment or greater.

Figure 11 is an image of unmodified muscovite and Figure 12 is an image of muscovite that was exposed to an aqueous HDTMA solution. The purpose of these images was to compare HDTMA sorbed on a well-understood, frequently imaged surface versus the lesser-studied and more variable natural clinoptilolite surface. The HDTMA on the surface of the muscovite appears as 2 types of features (Figure 12). Small, round features as well as regions of dendritic features are visible. The round features have an average diameter of about 6 nm. These are likely small clusters of HDTMA monomers. The height of the round features is between 0.2 and 0.4 nm, similar to the expected *z*-dimension of an HDTMA molecule at the surface. The dendritic features average 3.4 nm in width and 0.2 to 0.4 nm in height. These features are similar in dimension and form to those seen on the clinoptilolite modified to 12.5% and 25% of the ECEC. The *z*-dimensions compare favorably to the HDTMA molecule thickness calculated above.

Although the TMAFM images are from air-dry clinoptilolite samples, they give some indication of the

https://doi.org/10.1346/CCMN.1997.0450105 Published online by Cambridge University Press

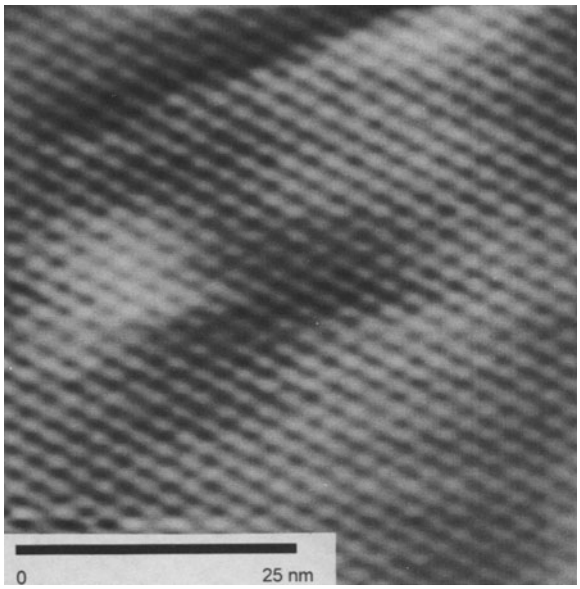

Figure 7. Unmodified clinoptilolite sample, 50-nm by 50-nm scale.

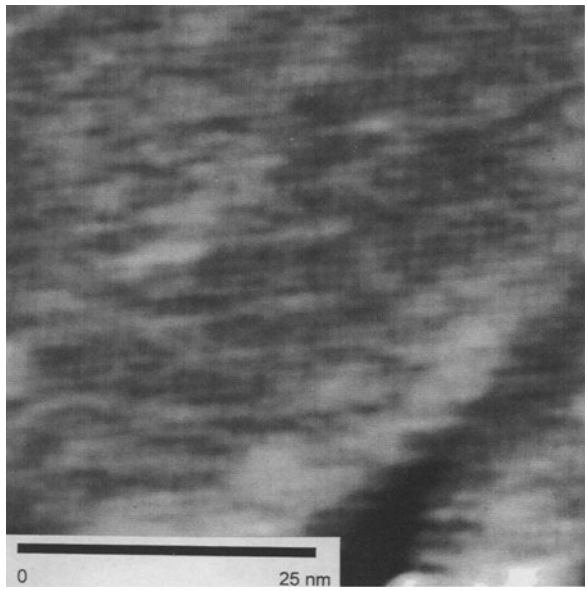

Figure 9. Clinoptilolite modified to 25% of ECEC with HDTMA, 50-nm by 50-nm scale.

topology of the surfactant-modified surface and the extent and conformation of HDTMA coverage on a small scale. Sorption of HDTMA on clinoptilolite is in clusters if the solution concentration is greater than the CMC. At lower loading (12.5%), the z-dimension of the HDTMA clusters is no greater than 1 HDTMA molecule diameter, indicating that rearrangement to a monolayer has occurred, and that the tail groups lie close to the clinoptilolite surface (Figure 1b). This is predicted by the model presented by Chen et al. (1992). At higher loading (25%), the z-dimension increases, indicating localized "stacking" or crossing of tail groups, and possibly buildup of a loose bilayer or admicelles. The images at all surfactant loadings show close association between the surfactant tails and the surface. At a surface loading rate of 70 meq/kg of HDTMA (100% of ECEC), the surfactant molecules would cover no less than 15.9 $m^2\ g^{-1}$, based solely on the head group van der Waals radius and ignoring any

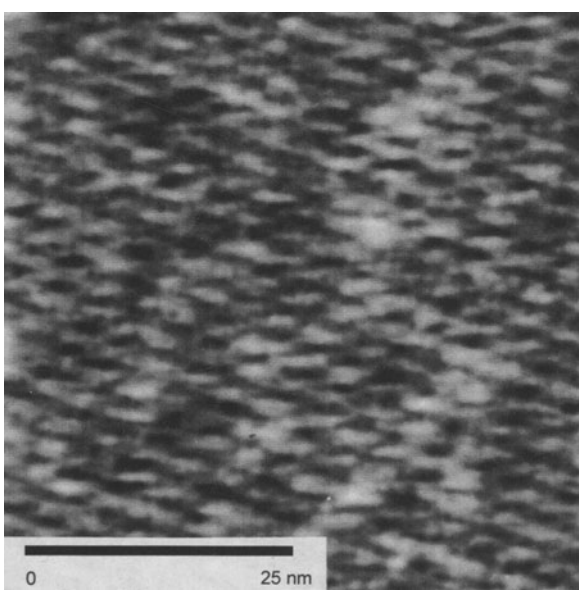

Figure 8. Clinoptilolite modified to 12.5% of ECEC with HDTMA, 50-nm by 50-nm scale.

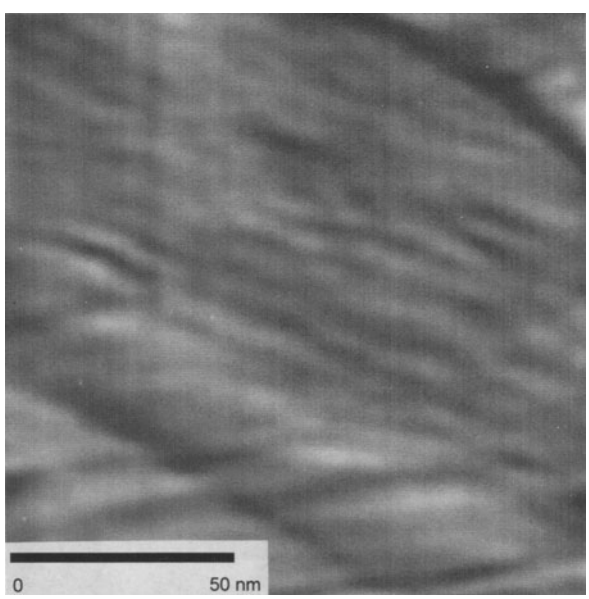

Figure 10. Clinoptilolite modified to 50% of ECEC with HDTMA (close-up of Figure 4, center section), 125-nm by 125-nm scale.

https://doi.org/10.1346/CCMN.1997.0450105 Published online by Cambridge University Press

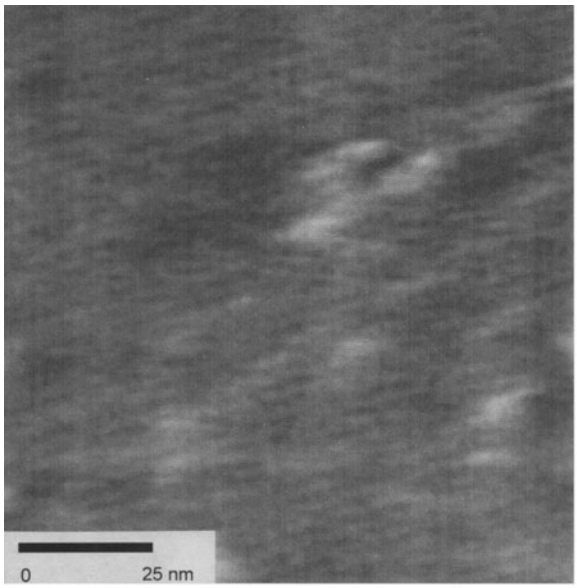

Figure 11. Unmodified muscovite mica sample, 100-nm by 100-nm scale.

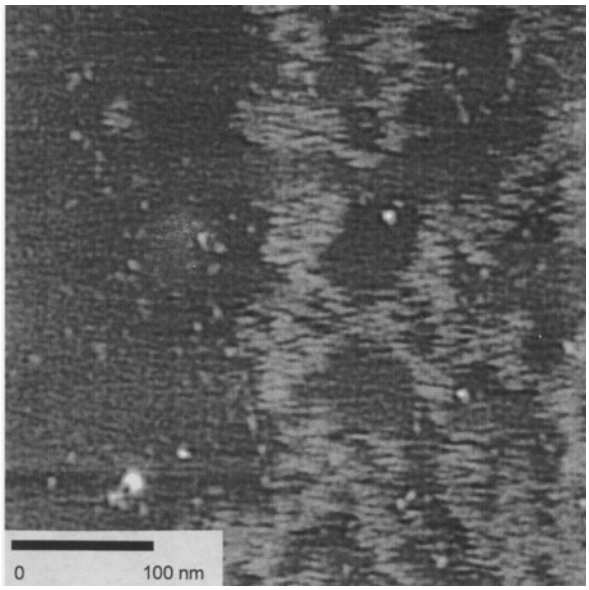

Figure 12. Muscovite mica exposed to an aqueous HDTMA solution, 100-nm by 100-nm scale.

space taken up by the tail groups (Israelachvili 1991). This molecular area is about the same as the available external surface area of 15.7 $m^2 g^{-1}$. At lower loading rates, the tail groups would probably take up space on the surface and overlap. Buildup of admicelles or some form of a bilayer is likely on these samples due to the spatial limitations of the surface. Another possibility is the buildup of cylindrical surfactant aggregates (Manne and Gaub 1995), which may account for the linear features in Figures 4, 8, 9 and 10.

Zhang et al. (1993) theorized that the stability of the HDTMA sorption to montmorillonite was due not only to cation-exchange effects but also was a function of the length of the tail group and the subsequent van der Waals forces between the tail and the surface. Entropic or hydrophobic forces also tend to exclude large hydrocarbon chains from the bulk water structure (Israelachvili 1991). HDTMA-modified clinoptilolite has been shown to be very stable even in the presence of high ionic strength solutions or organic solvents (Bowman et al. 1995). The above observations show that HDTMA sorption to clinoptilolite is a function of cation exchange, van der Waals forces and hydrophobic forces acting together.

HR-TGA results (see below) show that a significant amount of water was still absorbed to the external clinoptilolite surface during these room-temperature TMAFM measurements. The gravimetric water content of the unmodified and surfactant-modified zeolites changed from about 11% before to 7% after drying at 200 °C, based on the HR-TGA data below. The water lost below 200 °C can be assumed to be external surface water (D. L. Bish, Los Alamos National Laboratories, personal communication, 1995). Assuming a van der Waals radius for water of 0.0616 nm, the water content can be translated to more than 9 layers of water on the external surface of the clinoptilolite. Studies of organic vapor sorption onto mineral surfaces have indicated that surface water at thicknesses greater than 4 layers tends to behave more as bulk water than as structurally "fixed" water (Ong and Lion 1991; Petersen et al. 1995). The presence of this bulk water on the surface of the air-dry clinoptilolite implies that surfactant behavior in these studies may be similar to that for water-saturated systems.

TMAFM Probe-Surface Interactions

Changes in the set-point voltage, or tapping force, of the TMAFM probe may indicate surface changes. This is true if the probe used and the drive and root-mean-squared (RMS) amplitudes remain the same throughout and between images (K. Kjoller, Digital Instruments Corp., Santa Barbara, California, personal communication, 1995). The set point is an averaged value for an entire scan or set of scans and is most relevant to the total surface area scanned, rather than specific areas or features measured.

Surfactant buildup on the clinoptilolite surface produced increased repulsion of the silicon TMAFM probe. An increased set point was needed to provide enough voltage to allow the tip to contact the surface and overcome this repulsion. The mean set-point voltage for 5 different series of images is plotted as the mean and standard deviation vs. the HDTMA surface treatment level in Figure 13. A single probe was used sequentially on a minimum of 10 similarly modified samples for each series. Probes were changed between

https://doi.org/10.1346/CCMN.1997.0450105 Published online by Cambridge University Press

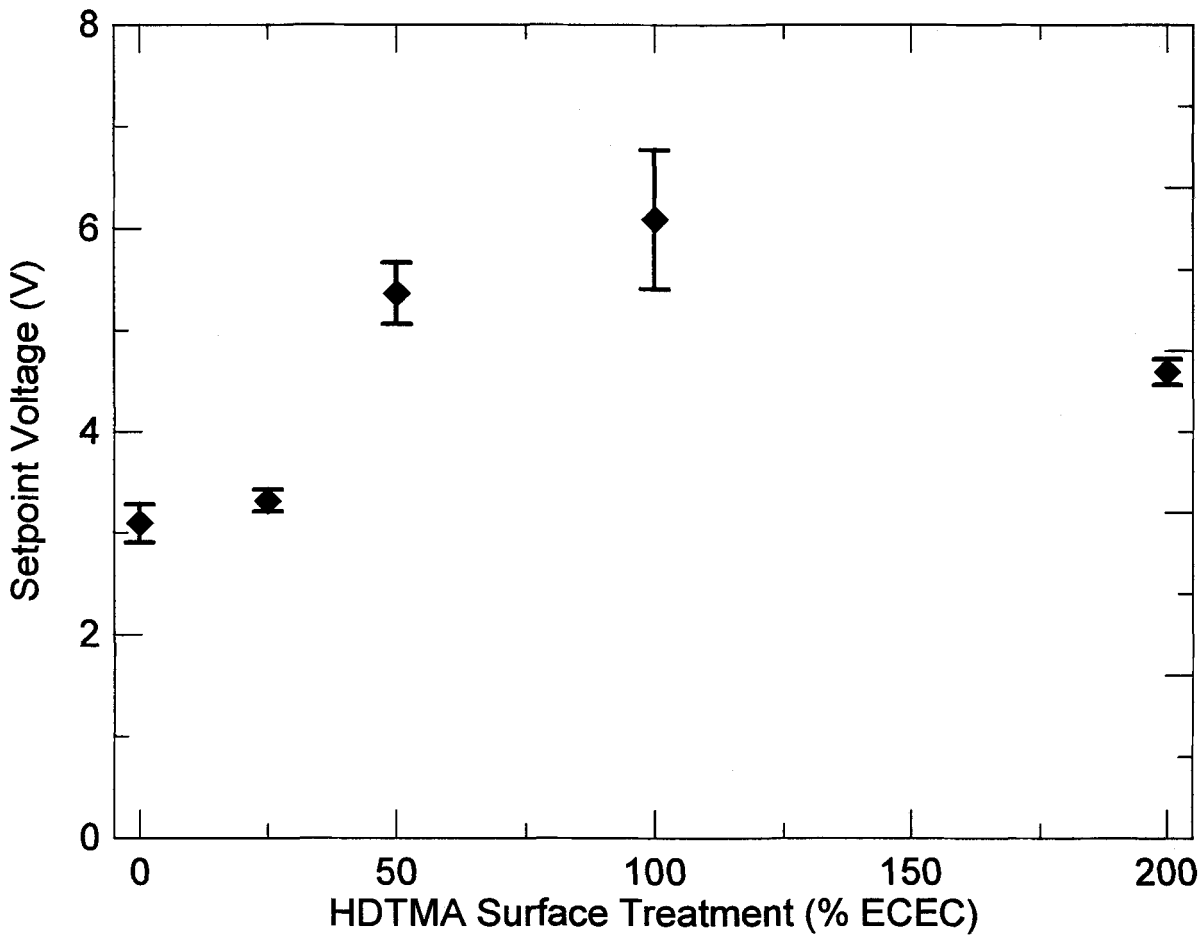

Figure 13. Mean set-point voltage for 5 different series of images, plotted as the mean and standard deviation versus the HDTMA surface treatment level.

samples modified at different loading levels, but the RMS amplitude was consistently set at zero and not changed throughout the series. The set-point voltage under these conditions was noted to increase from the 0% treatment level through the 25, 50, and 100% treatments (Figure 13), which was interpreted as an increase in average surface hydrophobicity. A decrease in the mean was noted for the 200% samples, probably due to a decrease in average surface hydrophobicity because of charge reversal on the surface with buildup of the surfactant and a change in surfactant orientation to expose hydrophilic head groups. Other explanations of the observed trend include increasing "softness" of the surface due to HDTMA buildup on the probe, or the presence of increasing amounts of water on the surface. A consistent downturn, however, for all samples at the 200% treatment level contraindicates the effect of "softness", because it is unlikely that these effects would have occurred at 200% and not on the 100% treatment samples, which appear very similar in the micrographs. HR-TGA results below indicate that water content is about the same for all samples, regardless of treatment level, and therefore attractive forces due to sorbed surface water should be approximately constant among all samples.

High-resolution Thermogravimetric Analysis

The results of the HR-TGA are shown as weight loss curves in Figure 14 and the accompanying derivative curves in Figure 15. The figures show weight losses for clinoptilolite, HDTMA and a series of HDTMA-modified clinoptilolite samples, from 25% to 200% of ECEC. Almost all of the weight of HDTMA bromide is lost upon heating to 232 °C and is seen clearly as a large, sharp peak in the derivative curve (Figure 15). A small amount of weight loss, about 11%, occurs for the unmodified clinoptilolite from 30 to 400 °C. This is due to water desorption (Bish 1988). In the weight loss curves (Figure 14) for the modified clinoptilolite, we observed a sequential loss of mass due to both water desorption and HDTMA pyrolysis and desorption. The 25% and 50% modifications showed similar behavior; however, replication of these treatments and TGA analyses yielded the same results.

https://doi.org/10.1346/CCMN.1997.0450105 Published online by Cambridge University Press

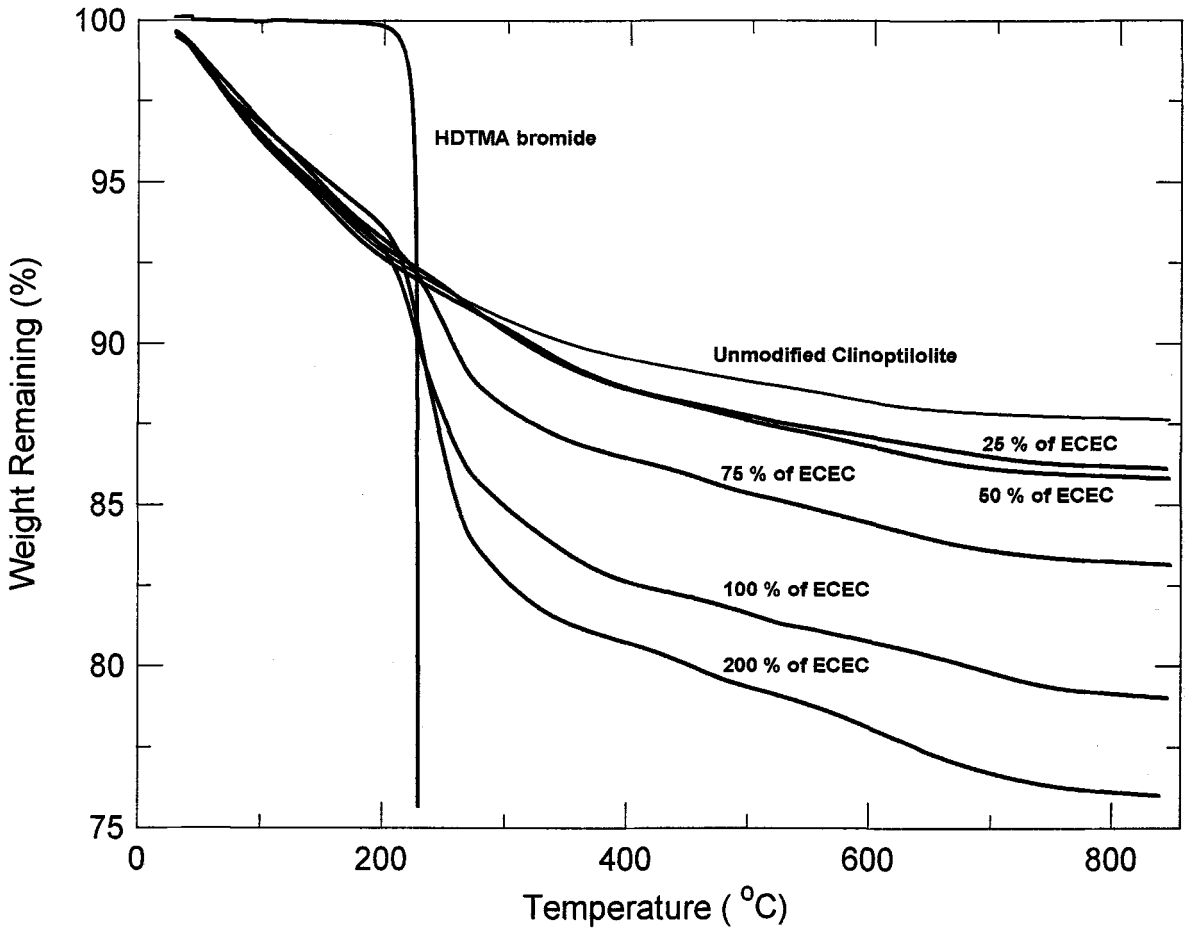

Figure 14. Weight-loss curves from HR-TGA analysis for unmodified clinoptilolite. HDTMA bromide and a series of HDTMA-modified clinoptilolites from 25% to 200% of ECEC.

In the derivative curves of the modified zeolites (Figure 15), the first water-loss peak occurs at about 50 °C, followed by a second water-loss peak at 159 °C. Further water loss is the cause of the continued gradual slope of the baselines to 800 °C (Bish 1988). No other peaks occur on the unmodified clinoptilolite curve. Weak, broad peaks at 265.6 °C and 334 °C are seen in the derivative curves for the 50%- and 25%-modified samples. These losses correspond to pyrolysis of HDTMA from higher-energy bonding sites, probably material that is closely bound to the clinoptilolite surface and is therefore stabilized with respect to pyrolysis. A stronger peak at 251.6 °C is seen for the 75%-treatment sample and is indicative of an intermediate bonding state of HDTMA, slightly less stabilized than seen for the lower loading levels. This peak underlies a shoulder evident in the 2 largest peaks, which correspond to HDTMA losses from the 100%- and 200%-modified samples. These large peaks are found at 230 °C, with the shoulder at 253.6 °C. The large peaks can be directly correlated with the unbonded HDTMA weight-loss derivative, and correspond to removal of HDTMA from lower-energy or less-stabilized bonding sites such as the external portion of a bilayer or admicelle. The HDTMA is held in those sites with weaker hydrophobic or van der Waals forces. This difference in pyrolysis temperature and peak breadth between the low and high loading levels indicates stronger, more complex bonding of HDTMA at lower treatment levels, presumably because of cation exchange or other chemical bonding effects in combination with van der Waals forces.

The above evidence from the TMAFM and HR-TGA correlates well with the surfactant sorption model proposed by Chen et al. (1992). Thickening of the surfactant layer beyond a monolayer and the presence of zones of surfactant coverage on the clinoptilolite surface at 25% of the ECEC and above indicates the possibility of the presence of rearranged admicelles at the lower treatment levels. The pyrolysis energy differences between higher treatment levels (>75%) and lower treatment levels (<75%) also indicate that admicelles or some form of a bilayer exist on the surface at less than 100% of the ECEC. This is consistent with

https://doi.org/10.1346/CCMN.1997.0450105 Published online by Cambridge University Press

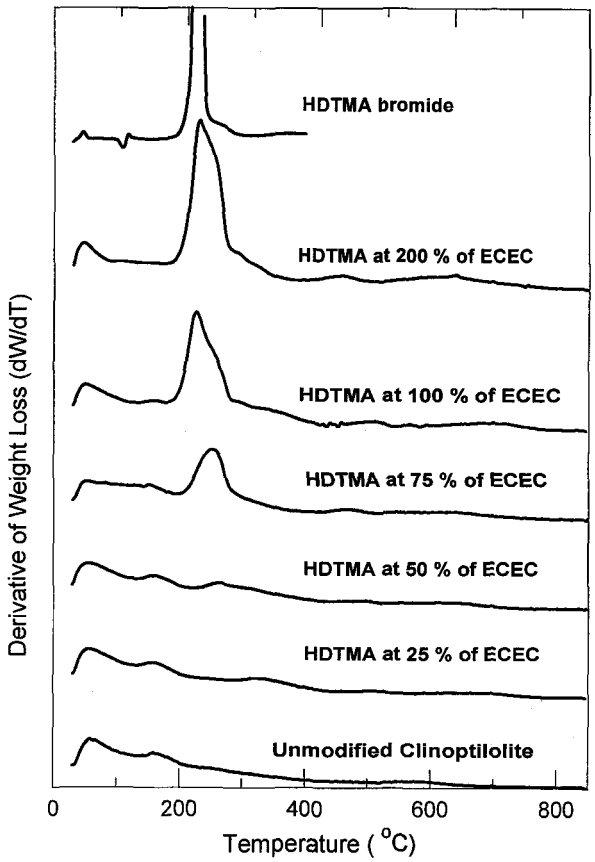

Figure 15. Derivative curves from the HR-TGA analysis for unmodified clinoptilolite, HDTMA bromide and a series of HDTMA-modified clinoptilolites from 25% to 200% of ECEC.

the TMAFM z-dimension measurements, which suggest multiple tail group buildup at as low as 25% loading. It also appears that, at low treatment levels, HDTMA sorption to the surface may be stabilized by van der Waals forces between the surfactant tail group and the clinoptilolite surface. This stabilization is probably very similar to that proposed for clays (Zhang et al. 1993).

SUMMARY AND CONCLUSIONS

TMAFM images were obtained in air for unmodified and surfactant-modified forms of microcrystalline clinoptilolite and for surfactant-modified muscovite. The molecular structure of the clinoptilolite is apparent in the higher-resolution images and compares well to previously reported fluid cell images of much larger, artificially cleaved crystals. Features of the surfactant noted on the clinoptilolite surface include a dendritic, clustered sorption pattern, which corresponds to agglomerations of surfactant molecules, and extensive coverage of the surface at low loading levels with near complete coverage at 50% of the ECEC. The z-dimension of the sorbed material is on the order of multiples of the average van der Waals diameter of a hydrocarbon chain. Overlap of chains suggested some form of admicelle or bilayer formation with increased coverage. Comparisons with HDTMA sorbed onto muscovite showed similarities between HDTMA conformation on the 2 mineral surfaces and yielded comparable measurements of surfactant cluster length and z-dimension. Comparisons of surfactant size, loading and available external surface area measurements show that the surfactant can cover the mineral surface extensively even when the equivalents of surfactant applied are less than 100% of the ECEC. Set-point voltage measurements indicated increased hydrophilicity of the surface at the 200% loading level, suggesting charge reversal.

HR-TGA results showed significant stabilization of HDTMA sorbed at 75% and lower loadings compared to that sorbed at higher loadings. This is due to the combined stabilization effects of coulombic and van der Waals forces between HDTMA and the clinoptilolite surface.

ACKNOWLEDGMENTS

This study was supported by a student research grant from The Clay Minerals Society, the Oak Ridge Institute for Science and Education research travel program, Waste-Management Education and Research Consortium (WERC) Grant No. 01-4-23190, contract DE-AC09-76SROO-819 between the US Department of Energy and the University of Georgia and by ERDA/WSRC subcontract AA46420T. The generous support of the Advanced Analytical Center for Environmental Sciences at the Savannah River Ecology Laboratory, including B. Teppen, J. Seaman and P. Bertsch is acknowledged. K. Nagy of Sandia National Laboratories provided valuable advice and review of the TMAFM images.

REFERENCES

Bish DL. 1988. Effects of composition on the dehydration behavior of clinoptilolite and heulandite. Kalló D, Sherry HS, editors. Occurrence, properties, and utilization of natural zeolites. Budapest, Hungary: Akadémiai Kiadó. p 565–576.

Bowman RS, Haggerty GM, Huddleston RG, Neel D, Flynn MM. 1995. Sorption of nonpolar organic compounds, inorganic cations, and inorganic oxyanions by surfactant-modified zeolites. Sabatini DA, Knox RC, Harwell JH, editors. Surfactant-enhanced subsurface remediation. ACS symposium series 594. Washington, DC: Am Chem Soc. p 54–64.

Brunauer S, Emmett PH, Teller E. 1938. Adsorption of gases in multimolecular layers. J Am Chem Soc 60:309–319.

Chen YL, Chen S, Frank C, Israelachvili J. 1992. Molecular mechanisms and kinetics during the self-assembly of surfactant layers. J Colloid Interface Sci 153(1):244–265.

Chipera SJ, Bish DL. 1995. Multireflection RIR and intensity normalizations for quantitative analyses: Applications to feldspars and zeolites. Powder Diffract 10:47–55.

Haggerty GM, Bowman RS. 1994. Sorption of chromate and other inorganic anions by organozeolite. Environ Sci Technol 28(3):452–458.

Israelachvili JN. 1991. Intermolecular and surface forces. 2nd ed. San Diego, CA: Academic Pr. 450 p.

Komiyama M, Yashima T. 1994. Atomic force microscopy images of natural zeolite surfaces observed under ambient conditions. Jpn J Appl Phys 33(1,6B):3761–3763.

MacDougall JE, Cox SD, Stucky GD, Weisenhorn AL, Hansma PK, Wise WS. 1991. Molecular resolution of zeolite surfaces as imaged by atomic force microscopy. Zeolites 11:429–433.

Malliaris A, Lang J, Zana R. 1986. Micellar aggregation numbers at high surfactant concentration. J Colloid Interface Sci 110(1):237–242.

Manne S, Gaub HE. 1995. Molecular organization of surfactants at solid-liquid interfaces. Science 270:1480–1482.

Maurice PA. 1995. Applications of atomic-force microscopy in mineral-water interface chemistry. American Chemical Society preprint extended abstract, Division of Environmental Chemistry; 1995 April 2–7; Anaheim, CA. p 521–524.

Ming DW, Dixon JB. 1987. Quantitative determination of clinoptilolite in soils by a cation-exchange capacity method. Clays Clay Miner 35:463–468.

Ming DW, Mumpton FA. 1989. Zeolites in soils. In: Dixon JB, Weed SB, editors. Minerals in soil environments. 2nd ed. Madison, WI: Soil Sci Soc Am. p 873–911.

Neel D, Bowman RS. 1992. Sorption of organics to surface-altered zeolites. Proc 36th Annu New Mexico Water Conf; Las Cruces; 1991 November 7–8. Las Cruces: New Mexico Water Research Inst. p 57–61.

Ong SK, Lion LW. 1991. Effects of soil properties and moisture on the sorption of trichloroethylene vapor. Water Res 25:29–36.

Petersen LW, Moldrup P, El-Farhan YH, Jacobsen OH, Rolston DE. 1995. The effect of moisture and soil texture on the adsorption of organic vapors. J Environ Qual 24:752–759.

Reiss-Husson F, Luzzati V. 1964. The structure of the micellar solutions of some amphiphilic compounds in pure water as determined by absolute small-angle X-ray scattering techniques. J Phys Chem 68:3504–3510.

Scandella L, Kruse N, Prins R. 1993. Imaging of zeolite surface structures by atomic force microscopy. Surf Sci Lett 281:331–334.

Smyth, JR, Spaid AT, Bish DL. 1990. Crystal structures of a natural and a Cs-exchanged clinoptilolite. Am Mineral 75:522–528.

Stipp SLS, Eggleston CM, Nielsen BS. 1994. Calcite surface structure observed at microtopographic and molecular scales with atomic force microscopy (AFM). Geochim Cosmochim Acta 58(14):3023–3033.

Sullivan EJ, Bowman RS, Haggerty GM. 1994. Sorption of inorganic oxyanions by surfactant-modified zeolite. Spectrum 94, Proc Nuclear and Hazardous Waste Management International Topical Meeting, vol 2; 1994 August 14–18; Atlanta, GA. p 940–945.

Weisenhorn AL, MacDougall JE, Gould AC, Cox SD, Wise WS, Massie J, Maivald P, Elings VB, Stucky GD, Hansma PK. 1991. Imaging and manipulating molecules on a zeolite surface with an atomic force microscope. Science 24: 1330–1333.

Zhang ZZ, Sparks DL, Scrivner NC. 1993. Sorption and desorption of quaternary amine cations on clays. Environ Sci Technol 27:1625–1631.

Zhong Q, Inniss D, Kjoller K, Elings VB. 1993. Fractured polymer/silica fiber surface studied by tapping mode atomic force microscopy. Surf Sci Lett 290:L688–L692.

(Received 20 November 1995; accepted 15 March 1996; Ms. 2717)